TECHNICAL RESEARCH REPORT

SYSTEMS RESEARCH CENTER

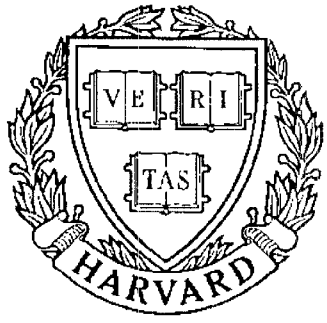

Supported by the National Science Foundation Engineering Research Center Program (NSFD CD 8803012), Industry and the University

On Image Deconvolution Using Multiple Sensors

by N. Sidiropoulos, J. Baras and C. Berenstein

TR 90-59

On Image Deconvolution Using Multiple Sensors *

N. Sidiropoulos† J. Baras‡ C. Berenstein§

Systems Research Center
University of Maryland
College Park, MD 20742
June 1990

Abstract

We consider the two dimensional Analytic Bezout Equation (ABE) and investigate the properties of a particular solution, based on certain conditions imposed on the convolution kernels. The results permit the reconstruction of the original signal using compactly supported deconvolution kernels. Arbitrarily good resolution (i.e. large bandwidth) can be achieved based solely upon computational resources. A number of implementation problems arising out of the need to approximate a basically infinite computation have been addressed and efficient Data Parallel grid layouts that perform the required computation have been designed.

Permission to publish this abstract seperately granted.

*Research partially supported by NSF grant NSFD CDR 8803012, through the Engineering Research Centers Program

†Also with the Department of Electrical Engineering

‡Also with the Department of Electrical Engineering

§Also with the Department of Mathematics

On Image Deconvolution Using Multiple Sensors *

N. Sidiropoulos† J. Baras‡ C. Berenstein§

Systems Research Center
University of Maryland
College Park, MD 20742
June 1990

Abstract

We consider the two dimensional Analytic Bezout Equation (ABE) and investigate the properties of a particular solution, based on certain conditions imposed on the convolution kernels. The results permit the reconstruction of the original signal using compactly supported deconvolution kernels. Arbitrarily good resolution (i.e. large bandwidth) can be achieved based solely upon computational resources. A number of implementation problems arising out of the need to approximate a basically infinite computation have been addressed and efficient Data Parallel grid layouts that perform the required computation have been designed.

*Research partially supported by NSF grant NSFD CDR 8803012, through the Engineering Research Centers Program

†Also with the Department of Electrical Engineering

‡Also with the Department of Electrical Engineering

§Also with the Department of Mathematics

1 Introduction

Signal deconvolution is a fundamental problem related to a variety of scientific and engineering disciplines. The traditional problem formulation can be stated as follows: we observe the output of a Linear Time Invariant system modelled by a convolution operator with known kernel (or convoluter) and wish to synthesize the input signal based on output observations. This is generally an ill-posed problem, and it does not admit a unique solution unless certain *a priori* assumptions are made. These assumptions can severely narrow the range of applications. Any physical device is band limited and thus high frequency information is lost whenever an input signal is observed through the device.

An alternative approach is to use *a family* of suitably chosen Linear Time Invariant convolution operators and attempt to reconstruct the input signal by combining the outputs of all available devices.

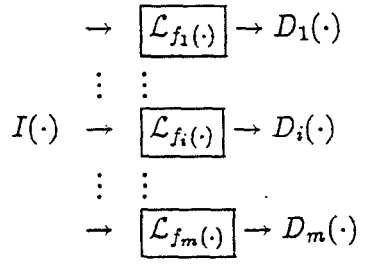

Figure 1: Multiple convolutional operators operating on a single input

Consider the system of figure 1. The $f_i's$ are distributions of compact support defined over $\mathcal{R}^n$ and $\mathcal{L}_{f_i}$ denotes convolution with kernel f_i. The natural question that comes up is: what is the minimum possible m and what conditions should the f_i's satisfy so that we can uniquely determine $I(\cdot)$ from the $D_i(\cdot)$? We are specifically interested in obtaining *linear* estimates of the input signal based on output observations from the bank of available devices. Mathematically the problem can be formulated as a convolution equation. We are looking for a family of *deconvolvers* $h_i(\cdot)$, $i = 1, \cdots, m$ such that:

$$D_1 * h_1 + \cdots + D_m * h_m = I \tag{1}$$

Alternatively, we need a family of entire analytic functions $\widehat{h}_i(\cdot)$, $i = 1, \cdots, m$

such that:

$$\hat{D}_1\hat{h}_1 + \cdots + \hat{D}_m\hat{h}_m = \hat{I} \tag{2}$$

Here $\hat{}$ denotes Fourier Transform. Now observe that:

$$\hat{D}_i = \hat{I}\hat{f}_i,\ i = 1, \ldots m \tag{3}$$

Therefore equation 2 above is equivalent to:

$$\hat{f}_1\hat{h}_1 + \cdots + \hat{f}_m\hat{h}_m = 1 \tag{4}$$

The later equation is known as the Analytic Bezout Equation (ABE). It is a well-known fact that the existence of a family of deconvolvers, $\{\hat{h}_1, \cdots, \hat{h}_m\}$ that solves the Bezout Equation is completely equivalent to a coprimeness condition on the part of the f_i's. Let us formalize by introducing some necessary definitions and presenting a number of important results.

Definition 1 *Let $\mathcal{E}'_{\mathcal{R}^n}$ denote the space of all distributions with compact support defined over $\mathcal{R}^n$. For convenience we drop the index $\mathcal{R}^n$ when the underlying space is obvious from the context.*

Let:

$$\hat{f}(\omega) \triangleq < f, e^{-i\omega t} > \tag{5}$$

$$\hat{f}(\omega) = \int_{-\infty}^{\infty} f(t)e^{-i\omega t}dt \tag{6}$$

Definition 2 *Let $\omega = (\omega_1, \cdots, \omega_n) \in C^n$. Then: $Im\omega = (Im\omega_1, \cdots, Im\omega_n)$, and define the function $p(\omega)$ as follows:*

$$p(\omega) \triangleq |Im\omega| + log(1 + |\omega|) \tag{7}$$

Definition 3 *(Paley-Wiener Space). Let $\hat{\mathcal{E}}'_{\mathcal{R}^n}$ denote the space of all functions $\hat{f}$ which are analytic in C^n and have the property that for some constants A, $B > 0$ the following inequality holds:*

$$|\hat{f}(\omega)| \leq Ae^{Bp(\omega)} \tag{8}$$

Theorem 1 *(Paley - Wiener) [14, page 21]. The mapping $\mathcal{E}'_{\mathcal{R}^n} \mapsto \hat{\mathcal{E}}'_{\mathcal{R}^n}$ given by equation (5) for all $f \in \mathcal{E}'_{\mathcal{R}^n}$, is 1-1 and onto the Paley-Wiener Space $\hat{\mathcal{E}}'_{\mathcal{R}^n}$. For convenience we drop the index $\mathcal{R}^n$ at all instances where the underlying space is clear from context.*

Theorem 1 enables us to work with entire analytic functions and equation (4) instead of distributions of compact support and equation (1).

Theorem 2 *[13] There exists a family of functions $\{\widehat{h}_1, \cdots, \widehat{h}_m\}$ in $\widehat{\mathcal{E}}'$ that solves the Bezout Equation iff the family of entire functions $\{\widehat{f}_1 \cdots, \widehat{f}_m\}$ in $\widehat{\mathcal{E}}'$ is strongly coprime, i.e.* iff: *$\sum_{j=1}^{m} |\widehat{f}_j(\omega)|^2 \geq e^{-cp(\omega)}, \forall \omega \in C^n$, for some constant c. The function $p(\omega)$ is the one in Definition 2.*

Thus the problem of recovering the input signal reduces to the problem of finding suitable distributions $\{f_1, \cdots, f_m\}$ or, alternatively, entire functions $\{\widehat{f}_1, \cdots, \widehat{f}_m\}$ in $\widehat{\mathcal{E}}'$ such that the coprimeness condition is satisfied *for the smallest possible m.* The reason why we are interested in the smallest possible m is that these distributions translate to actual devices, and it is usually desired to achieve reconstruction using the minimum possible number of devices.

Our approach is based on the work of C. Berenstein and A. Yger [1,2,5, 6,7,8] and [19]. The core of their research results, restricted to our present scope, is summarized in a theorem that we will introduce shortly, but before that let us give a number of definitions:

Definition 4 *Let K be a compact subset of $\mathcal{R}^n$. Define the* **supporting function** *of K as follows:*

$$H_K(\xi) \triangleq max\{x \cdot \xi | x \in K\} \tag{9}$$

where $\cdot$ denotes inner product and $\xi \in \mathcal{R}^n$.

Definition 5 *A family of n distributions $\{f_1, \ldots, f_n\}$ with compact support in $\mathcal{R}^n$ is* **well behaved** *if there exist positive constants A,B,N,K,C and two supporting functions H_o, H_1, such that $0 \leq H_o \leq H_1$, and such that the common zero set, $\mathcal{Z}$, of the functions $\{\widehat{f}_1, \cdots, \widehat{f}_n\}$ is almost real i.e. $\forall \omega \in \mathcal{Z} : |Im\omega| \leq C\, log(2 + |\omega|)$, and the number of zeros in $\mathcal{Z}$ included in an open ball of radius r grows like r^A : $n(\mathcal{Z}, r) = O(r^A)$. Furthermore, denoting:*

$$|\widehat{f}(z)| \triangleq \left[\Sigma_{i=1}^{n} |\widehat{f}_i(z)|^2\right]^{1/2} \tag{10}$$

the following inequality holds:

$$|\widehat{f}(z)| \geq \frac{B d(z, \mathcal{Z})^K e^{H_o(Imz)}}{(1 + |z|)^N} \tag{11}$$

where $d(z, \mathcal{Z})$ is the Euclidean distance of the point z from the set $\mathcal{Z}$. It can be shown that under these conditions the set $\mathcal{Z}$ is discrete, i.e. the points $\zeta \in \mathcal{Z}$ are isolated.

Definition 6 *A well-behaved family* $\{f_1, \cdots, f_n\}$ *is* **very well behaved** *if there exist constants* $M, C_1 > O$ *such that* $\forall \zeta \in \mathcal{Z}$ *we have that:*

$$|J(\zeta)| \triangleq |det[\frac{\partial \widehat{f}_j}{\partial z_i}(\zeta)]_{ij}| \geq C_1(1 + |\zeta|)^{-M} \tag{12}$$

This last condition guarantees that the points in $\mathcal{Z}$ (the set of common zeros of the family $\{\widehat{f}_1, \cdots, \widehat{f}_n\}$) are **well seperated**, i.e. there exist constants $M', C_2 > 0$ such that for any $\zeta \in \mathcal{Z}$ there exists $r = r(\zeta)$ such that

$$r(\zeta) \geq \frac{C_2}{(1 + |\zeta|)^{M'}}$$

and such that the open ball $B_r(\zeta)$ contains no other points in $\mathcal{Z}$. We now give a restricted version of a Theorem of C. Berenstein and A. Yger that is sufficient for our purposes and is simpler in the sense that it does not involve cumbersome notation, thus helping to keep things in perspective: Suppose $n = 2$ (i.e. we have distributions defined over $\mathcal{R}^2$) and $m = n + 1 = 3$ (i.e. we use 3 convolvers).

Theorem 3 *[8, Theorem 1 p.57] Let* $\{f_1, f_2, f_3\}$ *be a strongly coprime family of compactly supported distributions over* $\mathcal{R}^2$. *Suppose that the subfamily* $\{f_1, f_2\}$ *is very well behaved. Suppose* f_3 *is the "best" kernel in the sense that it has the smallest support of all three. Let* H_0, H_1 *be as in definition 5 for the subfamily* $\{f_1, f_2\}$. *Define*

$$H_2(\theta) = max_{1 \leq j \leq 3} max\{x \cdot \theta \ : x \in supp f_j\}, \ \theta \in \mathcal{R}^2$$

and suppose $H_2 \leq 2H_1$. *Furthermore suppose* $\exists \ r_o > 0 such that r_o|\theta| \leq 4H_o(\theta) - 2H_1(\theta) - H_2(\theta)$ *(these conditions control the support of* f_3 *vs. the support of* f_1, f_2*). Then for any* $u \in C_o^\infty(\mathcal{R}^2)$ *compactly supported and with "small" support:*

supp $u \subseteq \{x \in \mathcal{R}^n : |x| \leq r_0 \}$, *one can write:*

$$\widehat{u}(z) = \sum_{\zeta \in \mathcal{Z}} \frac{\widehat{u}(\zeta)}{J(\zeta)\widehat{f}_3(\zeta)} \begin{vmatrix} g_1^1(z,\zeta) & g_1^2(z,\zeta) & g_1^3(z,\zeta) \\ g_2^1(z,\zeta) & g_2^2(z,\zeta) & g_2^3(z,\zeta) \\ \widehat{f}_1(z) & \widehat{f}_2(z) & \widehat{f}_3(z) \end{vmatrix} \tag{13}$$

where $z = (z_1, z_2)$, $\zeta = (\zeta_1, \zeta_2)$, *both in* C^2, *and:*

$$g_1^i(z,\zeta) \triangleq \frac{\widehat{f}_i(z_1,\zeta_2) - \widehat{f}_i(\zeta_1,\zeta_2)}{z_1 - \zeta_1} \tag{14}$$

$$g_2^i(z,\zeta) \triangleq \frac{\widehat{f}_i(z_1,z_2) - \widehat{f}_i(z_1,\zeta_2)}{z_2 - \zeta_2} \tag{15}$$

and $J(\zeta) = det(M(z))|_{z=\zeta}$, *where the Jacobian matrix* $M(z)$ *is defined as:*

$$M(z) \triangleq \begin{bmatrix} \frac{\partial \widehat{f}_1}{\partial z_1} & \frac{\partial \widehat{f}_2}{\partial z_1} \\ \frac{\partial \widehat{f}_1}{\partial z_2} & \frac{\partial \widehat{f}_2}{\partial z_2} \end{bmatrix} \tag{16}$$

and:

$$\mathcal{Z} = \{z \in C^2 : \widehat{f}_1(z) = \widehat{f}_2(z) = 0\} \tag{17}$$

Remarks: The result obviously extends to higher-dimensional spaces, see [8]. Equation (13) is an interpolation formula since it constructs the entire function $\widehat{u}(\cdot)$ based on distinct point values of $\widehat{u}(\cdot)$ at a discrete set of well seperated points in the plane. The significance of Theorem 3 can be demonstrated by a simple manipulation of equation (13), which can be rewritten in the form:

$$\widehat{u}(z) = \widehat{h_1}(z)\widehat{f_1}(z) + \widehat{h_2}(z)\widehat{f_2}(z) + \widehat{h_3}(z)\widehat{f_3}(z) \tag{18}$$

And since $u(x)$ is of sufficiently small support (we can certainly shrink the support of u below r_o) then $\widehat{u}(z) \cong 1$ and:

$$1 \cong \widehat{h_1}(z)\widehat{f_1}(z) + \widehat{h_2}(z)\widehat{f_2}(z) + \widehat{h_3}(z)\widehat{f_3}(z)$$

i.e. $\{\widehat{h}_1(z), \widehat{h}_2(z), \widehat{h}_3\}$ give an approximate solution to the ABE. In principle we can set $u = \delta$ thus getting $\widehat{u}(\cdot) = 1$ and obtain *exact* deconvolvers. Notice that $\widehat{u}(\cdot)$ *is not* compactly supported (because u *is* compactly supported). Observe that since a realistic computation will truncate the sum over $\mathcal{Z}$ in equation (13) to make it finite, it will force $\widehat{u}(\cdot)$ to be zero on the discrete set $\mathcal{Z} \cap \{\zeta : \|\zeta\| > \zeta_0\}$, for some finite ζ_0. We will discuss this point in detail later on. For the moment let us consider a specific model problem.

2 Model Problem

Let χ_K denote the characteristic function of the compact set $K \subset \mathcal{R}^n$ and consider the following family of convolution kernels:

$$f_1(t_1,t_2) = \chi_{[-\sqrt{3},\sqrt{3}]\times[-\sqrt{3},\sqrt{3}]}(t_1,t_2) \tag{19}$$

$$f_2(t_1,t_2) = \chi_{[-\sqrt{2},\sqrt{2}]\times[-\sqrt{2},\sqrt{2}]}(t_1,t_2) \tag{20}$$

$$f_3(t_1,t_2) = \chi_{[-1,1]\times[-1,1]}(t_1,t_2) \tag{21}$$

with Fourier transforms given by

$$\widehat{f}_1(z_1,z_2) = \frac{4}{z_1 z_2}\sin(\sqrt{3}z_1)\sin(\sqrt{3}z_2) \tag{22}$$

$$\widehat{f}_2(z_1,z_2) = \frac{4}{z_1 z_2}\sin(\sqrt{2}z_1)\sin(\sqrt{2}z_2) \tag{23}$$

$$\widehat{f}_3(z_1,z_2) = \frac{4}{z_1 z_2}\sin(z_1)\sin(z_2) \tag{24}$$

Then it is easy to verify that $\{f_1, f_2, f_3\}$ satisfy all conditions of theorem 3. Here

$$\mathcal{Z} = \left\{\left(\frac{j\pi}{\sqrt{3}},\frac{k\pi}{\sqrt{2}}\right)\ ,\ k,j = \pm 1,\pm 2,\cdots\right\}\cup\left\{\left(\frac{j\pi}{\sqrt{2}},\frac{k\pi}{\sqrt{3}}\right)\ ,\ k,j = \pm 1,\pm 2,\cdots\right\} \tag{25}$$

$$J(\zeta) = \begin{vmatrix} \frac{4\sin(\sqrt{3}\zeta_2)}{\zeta_1^2\zeta_2}r_1(\zeta_1) & \frac{4\sin(\sqrt{2}\zeta_2)}{\zeta_1^2\zeta_2}r_2(\zeta_1) \\ \frac{4\sin(\sqrt{3}\zeta_1)}{\zeta_2^2\zeta_1}r_1(\zeta_2) & \frac{4\sin(\sqrt{2}\zeta_1)}{\zeta_2^2\zeta_1}r_2(\zeta_2) \end{vmatrix} \tag{26}$$

with

$$r_1(x) \triangleq \sqrt{3}x\cos(\sqrt{3}x) - \sin(\sqrt{3}x) \tag{27}$$

$$r_2(x) \triangleq \sqrt{2}x\cos(\sqrt{2}x) - \sin(\sqrt{2}x) \tag{28}$$

and after a series of transformations we can rewrite equation (13) in the form of equation (18) and then read out the expressions for $\widehat{h}_1$, $\widehat{h}_2$, $\widehat{h}_3$. These are given by the infinite sums:

$$\widehat{h}_i(z_1,z_2) = \sum_{\zeta\in\mathcal{Z}} \frac{\widehat{u}(\zeta)}{J(\zeta)\widehat{f}_3(\zeta)} \cdot \frac{C_i(z,\zeta)}{(z_1-\zeta_1)(z_2-\zeta_2)} \tag{29}$$

with

$$\begin{aligned} C_1(z,\zeta) \triangleq\ & \widehat{f}_2(z_1,\zeta_2)\left[\widehat{f}_3(z_1,z_2)-\widehat{f}_3(\zeta_1,\zeta_2)\right] - \\ & \widehat{f}_2(z_1,z_2)\left[\widehat{f}_3(z_1,\zeta_2)-\widehat{f}_3(\zeta_1,\zeta_2)\right] \end{aligned} \tag{30}$$

$$\begin{aligned} C_2(z,\zeta) \triangleq\ & \widehat{f}_1(z_1,z_2)\left[\widehat{f}_3(z_1,\zeta_2)-\widehat{f}_3(\zeta_1,\zeta_2)\right] - \\ & \widehat{f}_1(z_1,\zeta_2)\left[\widehat{f}_3(\zeta_1,\zeta_2)-\widehat{f}_3(z_1,z_2)\right] \end{aligned} \tag{31}$$

$$C_3(z,\zeta) \triangleq \widehat{f}_1(z_1,\zeta_2)\widehat{f}_2(z_1,z_2) - \widehat{f}_1(z_1,z_2)\widehat{f}_2(z_1,\zeta_2) \tag{32}$$

Definition 7 *The function* $\mathcal{F}(\cdot,\cdot)$ *is* **symmetric** *iff*
$\mathcal{F}(z_1,z_2) = \mathcal{F}(-z_1,z_2)$, $\forall z_1,z_2 \in \mathcal{C}^2$
and
$\mathcal{F}(z_1,z_2) = \mathcal{F}(z_1,-z_2)$, $\forall z_1,z_2 \in \mathcal{C}^2$.

Definition 8 *The function* $\mathcal{F}(\cdot,\cdot)$ *is* $\frac{\pi}{2}$ **rotation-invariant** *(* $\frac{\pi}{2}-ri$ *) iff*
$\mathcal{F}(z_1,z_2) = \mathcal{F}(z_2,z_1)$, $\forall z_1,z_2 \in \mathcal{C}^2$.

Notice that $\widehat{f}_1$, $\widehat{f}_2$, $\widehat{f}_3$ are all $\frac{\pi}{2}$-ri. Nevertheless the C_i's *are not*; for example $C_1(z_1,z_2) \neq C_1(z_2,z_1)$. Hence, in general, every *finite* approximation to $\widehat{h}_1$ will not be $\frac{\pi}{2}$-ri. In the limiting case we expect this bias to die out because of cancellations. Similar remarks hold for $\widehat{h}_2, \widehat{h}_3$. This fact will prove annoying for applications. A final remark is in order: The distributions $h_i = F.T.^{-1}\{\widehat{h}_i\}$ $i = 1,2,3$, where the $\widehat{h}_i's$ are those obtained using theorem 3 , are *compactly supported* (in fact of support comparable to that of the kernels f_i) . Thus, once obtained, they are easily realized *exactly* with finite delay (exactly refers to the fact that there is no need for truncation of their duration; sampling and finite word length arithmetic errors can be controlled to meet the design goals [21]). This property of these deconvolvers is their most desirable feature when compared to Wiener deconvolvers [1].

2.1 Exploitation of symmetries in the frequency domain

We are interested in ways to exploit inherent problem symmetry in order to reduce the computational complexity and improve arithmetic error performance. Consider the result obtained in equation (29) , which we rewrite here making the number of frequency variables explicit:

$$\widehat{h}_1(z_1,z_2) = \sum_{(\zeta_1,\zeta_2)\in\mathcal{Z}} \frac{\widehat{u}(\zeta_1,\zeta_2)}{J(\zeta_1,\zeta_2)\cdot\widehat{f}_3(\zeta_1,\zeta_2)} \cdot \frac{C_1(z_1,z_2,\zeta_1,\zeta_2)}{(z_1-\zeta_1)\cdot(z_2-\zeta_2)} \tag{33}$$

Assume that $\widehat{u}(\zeta_1,\zeta_2)$ is an even function of both its arguments. We will use the following notation to denote this: $\widehat{u}(\zeta_1,\zeta_2) \sim e(\zeta_1,\zeta_2)$. Similarly odd functions are denoted by $\sim o(\cdot)$. We are interested in symmetries in terms of (ζ_1,ζ_2) of the summation terms in equation (33) .

Let

$$W(z_1,z_2,\zeta_1,\zeta_2) \triangleq \frac{\widehat{u}(\zeta_1,\zeta_2)\cdot C_1(z_1,z_2,\zeta_1,\zeta_2)}{J(\zeta_1,\zeta_2)\cdot\widehat{f}_3(\zeta_1,\zeta_2)} \tag{34}$$

and recalling that

$$\mathcal{Z} = \left\{\left(\frac{j\pi}{\sqrt{3}},\frac{k\pi}{\sqrt{2}}\right)\ ,\ k,j=\pm1,\pm2,\cdots\right\}\cup\left\{\left(\frac{j\pi}{\sqrt{2}},\frac{k\pi}{\sqrt{3}}\right)\ ,\ k,j=\pm1,\pm2,\cdots\right\} \tag{35}$$

observe that

$$(n_1,n_2)\in\mathcal{Z} \longrightarrow (-n_1,n_2),\ (n_1,-n_2),\ (-n_1,-n_2)\in\mathcal{Z}$$

Now, for z fixed $C_1(z_1,z_2,\zeta_1,\zeta_2) \sim e(\zeta_1,\zeta_2)$ and $J(\zeta_1,\zeta_2) \sim o(\zeta_1)o(\zeta_2)$. Furthermore $\widehat{f}_3(\zeta_1,\zeta_2) \sim e(\zeta_1)e(\zeta_2)$. Thus

$$W(z_1,z_2,\zeta_1,\zeta_2) \sim o(\zeta_1)o(\zeta_2)$$

Therefore, for fixed z, the pointwise contribution of the four zeros:

$$(n_1,n_2),\ (-n_1,n_2),\ (n_1,-n_2),\ (-n_1,-n_2)$$

can be combined as follows:

$$W(z_1,z_2,n_1,n_2) \cdot \left[\frac{1}{(z_1-n_1)\cdot(z_2-n_2)} - \frac{1}{(z_1+n_1)\cdot(z_2-n_2)}\right] -$$

$$W(z_1,z_2,n_1,n_2) \cdot \left[\frac{1}{(z_1-n_1)\cdot(z_2+n_2)} - \frac{1}{(z_1+n_1)\cdot(z_2+n_2)}\right] =$$

$$= W(z_1,z_2,n_1,n_2)\cdot\frac{4\cdot n_1\cdot n_2}{(z_1^2-n_1^2)\cdot(z_2^2-n_2^2)}$$

Therefore we can combine the four individual contributions into a single term. Furthermore, notice that since for fixed z, $C_1(z_1, z_2, \zeta_1, \zeta_2) \sim e(z_1, z_2)$ this implies that $W(z_1, z_2, \zeta_1, \zeta_2) \sim e(z_1, z_2)$, thus the combined term above is $\sim e(z_1, z_2)$. Hence $\widehat{h}_1(z_1, z_2) \sim e(z_1, z_2)$, as the sum of even functions of both z_1 and z_2. Therefore we only need to compute the upper right quadrant of the Fourier transform plane. Notice that we have achieved combined savings (in the number of terms that need to be computed by any digital approximation scheme) of 1/16. This can make an enormous difference in any practical computation.

2.2 Windowing and Averaging

Our goal is the pointwise evaluation of the F.T. of approximate deconvolution kernels over a suitably chosen finite grid. For ease of reference we reproduce the formula obtained earlier (c.f. equation (29)):

$$\widehat{h}_i(z_1, z_2) = \sum_{(\zeta_1, \zeta_2) \in \mathcal{Z}} \frac{\widehat{u}(\zeta_1, \zeta_2)}{J(\zeta_1, \zeta_2) \cdot \widehat{f}_3(\zeta_1, \zeta_2)} \cdot \frac{C_i(z_1, z_2, \zeta_1, \zeta_2)}{(z_1 - \zeta_1) \cdot (z_2 - \zeta_2)} \tag{36}$$

Clearly this involves the pointwise (in z) computation of an infinite sum. Therefore, one way or another, we will have to truncate this sum at some point. This is equivalent to forcing $\widehat{u}(\zeta)$ to be zero on a set $\mathcal{Z} \cap \{\zeta : \|\zeta\| > \zeta_0\}$ for some finite ζ_0. Since each term of the sum in equation (36) is the Fourier transform of a compactly supported kernel this amounts to approximating h_i with a kernel $\widetilde{h}_i$ that is compactly supported but of wider support than h_i. Hence, we must strike a balance between computational feasibility and the size of the support of h_i in order to obtain meaningful results. Notice that in principle $u(t)$ can by anything as long as it is sufficiently compactly supported. Also note that *u(t) is the impulse response of the overall system that is realized* and thus $\widehat{u}(z)$ is the frequency response of the overall system. Clearly we would like u(t) to be as close to $\delta(t)$ as possible (in the sense of distributions) or, equivalently, $\widehat{u}(z)$ to be as close to unity as possible. This means that we would like to include as many terms as possible in (36). Observe that for fixed z the summation term corresponding to the point $\zeta \in \mathcal{Z}$, that is closest (in Euclidean distance) to z, is of significant magnitude. Therefore we should include all terms corresponding to points $\zeta \in \mathcal{Z}$ located within the desired bandwidth (and in fact many more). On the other hand, noise considerations dictate a *smooth* choice of u(t) which in turn implies a fast decay of $\widehat{u}(z)$ at infinity. Thus we have to accommodate

conflicting interests. We seek a compromise in the choice of $\widehat{u}(z)$ that will account for the following requirements:

1. $u(t)$ is sufficiently compactly supported (i.e. the condition of Theorem 3 is approximately satisfied).

2. $\widehat{u}(z)$ is close to the identity over some bounded region of interest (i.e. bandwidth requirements are being met).

3. $u(t)$ is sufficiently smooth (Noise averaging)

These requirements are clearly interrelated. It is not at all clear what is a proper choice for $\widehat{u}$. We have used functions of the form:

$$\widehat{u}(z) = \left(\prod_{i=1}^{2} \frac{\sin(\frac{\epsilon_i}{N} z_i)}{\frac{\epsilon_i}{N} z_i} \right)^N \cdot p_r(z) \tag{37}$$

where N is a small positive integer and ϵ_1, ϵ_2 are small positive reals. The function $p_r(z)$ is defined as follows:

$$p_r(z) = \begin{cases} 1, & |z_i| \leq r \ , \ i = 1,2 \\ 0, & elsewhere \end{cases} \tag{38}$$

The first factor is a two dimensional sinc-like function. This approach comes from experimentation and an attempt to control the residue in equation (36) due to the widening of the support of h_i. Here the parameter r (forced cutoff in rads/sec) is to be chosen sufficiently large to include all main features of the first factor (the main lobe and the principal sidelobes at least) , while keeping the size of the computation reasonable. If we fix ϵ and increase N then u gets smoother and its peak gets taller while its support remains fixed and the main lobe of $\widehat{u}$ gets wider. An undesirable result is that the amplitude within the main lobe of $\widehat{u}$ flattens out. On the other hand if we fix N and decrease ϵ the support of u narrows, its peak gets taller, and the main lobe of $\widehat{u}$ widens. Furthermore the main lobe amplitudes are pushed up towards unity. Simulation results are given at the end of this section . For the case $\epsilon_1 = \epsilon_2 = \epsilon$ we observe a high degree of energy concentration along a ribbon-like neighborhood of the z_2 axis, while amplitudes everywhere else are attenuated by at least an order of magnitude. This is not suprising because we have noted that any *finite* approximation to the deconvolution kernels *is not* $\frac{\pi}{2}$ *– rotation invariant.* Since we achieve better bandwidth

characteristics along z_2 we should choose ϵ_1 smaller than ϵ_2 (observe that the magnitude of the main lobe is $\sim \frac{1}{\epsilon}$). This will partially compensate for the problem by essentially spreading out the energy originally concentrated along the neighborhood of z_2.

The simulation results make clear that the bias against one frequency variable resulting from finite approximations of the proposed deconvolution kernels actually manifests itself in a profound way and can severely distort the overall system spectrum even at frequencies in the vicinity of the origin. There exists no a priori reason for the appearance of such a bias (for the particular model at hand is symmetric and $\frac{\pi}{2}$-ri) but rather the cause can be traced back to a somewhat arbitrary choice between two distinct possibilities in writing down interpolation formulas. Before we discuss this very important point let us give a partial "a posteriori" solution: if the transforms of the convolvers are symmetric and $\frac{\pi}{2}$-rotation invariant then a simple solution would be the following:

Let $\widehat{h}_{i,n}(z_1, z_2)$, $i = 1, 2, 3$ denote the obtained approximations of the Fourier transforms of the deconvolution kernels, where n denotes the cardinality of the nullset, $\mathcal{Z}_n$, over which we sum. Next for $i = 1, 2, 3$ define

$$\widehat{h}^L_{i,n}(z_1, z_2) \triangleq \widehat{h}_{i,n}(z_2, z_1) \tag{39}$$

and

$$\widehat{h}^*_{i,n}(z_1, z_2) \triangleq \frac{\widehat{h}_{i,n}(z_1, z_2) + \widehat{h}^L_{i,n}(z_1, z_2)}{2} \tag{40}$$

By definition $\widehat{h}^*_{i,n}(\cdot, \cdot)$ is $\frac{\pi}{2}$ rotation invariant since

$$\begin{aligned} \widehat{h}^*_{i,n}(z_2, z_1) &\triangleq \frac{\widehat{h}_{i,n}(z_2, z_1) + \widehat{h}^L_{i,n}(z_2, z_1)}{2} \\ &= \frac{\widehat{h}^L_{i,n}(z_1, z_2) + \widehat{h}_{i,n}(z_1, z_2)}{2} \\ &= \widehat{h}^*_{i,n}(z_1, z_2) \end{aligned} \tag{41}$$

Let $\widetilde{h}_i$, $i = 1, 2, 3$ denote the Fourier transforms of the exact deconvolution kernels. Then by theorem 3 we have that:

$$\widehat{h}_{i,n} \longrightarrow \widetilde{h}_i, \ as \ n \longrightarrow \infty, \ for \ i = 1, 2, 3 \tag{42}$$

Thus, by symmetry and $\frac{\pi}{2}$ rotation invariance of the solution:

$$\widehat{h}_{i,n}^{L} \longrightarrow \widetilde{h}_{i}^{L} \equiv \widetilde{h}_{i},\ as\ n \longrightarrow \infty,\ for\ i = 1,2,3 \tag{43}$$

Hence the same is true for their average, i.e. the family $\{\widehat{h}_{i,n}^{*};\ i = 1,2,3\}$ constitutes a converging solution. Furthermore for all finite n the later family behaves better because it acquires bandwidth in a radially increasing fashion. Simulation results for this averaged solution are given at the end of this section.

We now turn to the general case where the Fourier transforms of the convolvers are not symmetric and $\frac{\pi}{2}$ - rotation invariant. In this case it is not necessarily true that $\widetilde{h}_{i}^{L} \equiv \widetilde{h}_{i}$ and the remedy above fails. In fact *we expect* the exact solutions to be asymmetric and/or biased. Nevertheless we have to account for spurious responses introduced by the need to come up with a finite computation because otherwise the results will be severely distorted. We now investigate the cause of these problems and proceed to propose a definitive solution. Consider the determinant involved in the interpolation formula (13) of Theorem 3 .

$$d = \begin{vmatrix} g_1^1(z,\zeta) & g_1^2(z,\zeta) & g_1^3(z,\zeta) \\ g_2^1(z,\zeta) & g_2^2(z,\zeta) & g_2^3(z,\zeta) \\ \widehat{f}_1(z) & \widehat{f}_2(z) & \widehat{f}_3(z) \end{vmatrix} \tag{44}$$

where the $g_j^i(z,\zeta),\ i = 1,2,3\ ,\ j = 1,2$ are holomorphic functions given by

$$g_1^i(z,\zeta) = \frac{\widehat{f}_i(z_1,\zeta_2) - \widehat{f}_i(\zeta_1,\zeta_2)}{z_1 - \zeta_1} \tag{45}$$

$$g_2^i(z,\zeta) = \frac{\widehat{f}_i(z_1,z_2) - \widehat{f}_i(z_1,\zeta_2)}{z_2 - \zeta_2} \tag{46}$$

Now consider the first column of d. The idea is to write [8]

$$\widehat{f}_1(z_1,z_2) - \widehat{f}_1(\zeta_1,\zeta_2) = (z_1 - \zeta_1)\cdot g_1^1(z,\zeta) + (z_2 - \zeta_2)\cdot g_2^1(z,\zeta) \tag{47}$$

Quite clearly this can also be achieved via

$$\widehat{f}_1(z_1,z_2) - \widehat{f}_1(\zeta_1,\zeta_2) = (z_1 - \zeta_1)\cdot \bar{g}_1^1(z,\zeta) + (z_2 - \zeta_2)\cdot \bar{g}_2^1(z,\zeta) \tag{48}$$

Where $\bar{g}_1^1(z,\zeta)$ and $\bar{g}_2^1(z,\zeta)$ are defined as follows:

$$\bar{g}_1^1(z,\zeta) \triangleq \frac{\widehat{f}_1(z_1,z_2) - \widehat{f}_1(\zeta_1,z_2)}{z_1 - \zeta_1} \tag{49}$$

$$\bar{g}_2^1(z,\zeta) \triangleq \frac{\widehat{f}_1(\zeta_1,z_2) - \widehat{f}_1(\zeta_1,\zeta_2)}{z_2 - \zeta_2} \tag{50}$$

There is no *a priori* reason for choosing any particular holomorphic form; either will do. Nevertheless *some* choice has to be made. In the limit this choice makes no difference, but for all finite $n = \#\mathcal{Z}$, since *either* expansion pair of holomorphic functions is biased, the overall system response is biased towards one of the two frequency variables. Therefore we can define:

$$\bar{d} = \begin{vmatrix} \bar{g}_1^1(z,\zeta) & \bar{g}_1^2(z,\zeta) & \bar{g}_1^3(z,\zeta) \\ \bar{g}_2^1(z,\zeta) & \bar{g}_2^2(z,\zeta) & \bar{g}_2^3(z,\zeta) \\ \widehat{f}_1(z) & \widehat{f}_2(z) & \widehat{f}_3(z) \end{vmatrix} \tag{51}$$

with $\bar{g}_1^2$, $\bar{g}_2^2$, $\bar{g}_1^3$, $\bar{g}_2^3$ defined as follows

$$\bar{g}_1^2(z,\zeta) = \frac{\widehat{f}_2(z_1,z_2) - \widehat{f}_2(\zeta_1,z_2)}{z_1 - \zeta_1} \tag{52}$$

$$\bar{g}_2^2(z,\zeta) = \frac{\widehat{f}_2(\zeta_1,z_2) - \widehat{f}_2(\zeta_1,\zeta_2)}{z_2 - \zeta_2} \tag{53}$$

$$\bar{g}_1^3(z,\zeta) = \frac{\widehat{f}_3(z_1,z_2) - \widehat{f}_3(\zeta_1,z_2)}{z_1 - \zeta_1} \tag{54}$$

$$\bar{g}_2^3(z,\zeta) = \frac{\widehat{f}_3(\zeta_1,z_2) - \widehat{f}_3(\zeta_1,\zeta_2)}{z_2 - \zeta_2} \tag{55}$$

So we need to use equation (13) to obtain two sets of solutions: one using the original d, and one using $\bar{d}$ in place of d. Again since both solutions converge to the exact deconvolvers as $n \longrightarrow \infty$ the same is true for their average. Furthermore, the bias is canceled out and does not appear in the overall system spectrum. Observe that if the transforms of the convolvers are symmetric and $\frac{\pi}{2}$- rotation invariant this approach reduces to the much simpler *a posteriori* remedy discussed earlier, which requires about half as much computation.

Simulation results are presented in the sequence of figures that follows. A nullset cardinality $n = \#\mathcal{Z} = 3200$ points, a frequency step of 0.1718 rads/sec and a frequency resolution of 256×256 points is adopted throughout the whole sequence of simulations. The parameter t denotes threshold value. The magnitude of the Fourier transform of the convolution kernels

for the model problem is plotted in figures 2, 3, 4. The magnitude of the Fourier ransform of the overall system (i.e. bank of convolvers followed by bank of associated deconvolvers whose outputs are summed up to produce the overall system output) using the $\widehat{u}(z)$ given by equation (37) with parameters $\epsilon_1 = \epsilon_2 = \epsilon = 0.1$, $N = 3$ is plotted in figures 5, 6, 7 for various threshold levels. The following three figures, 8, 9, 10 depict the magnitude of the Fourier transform of the overall system using the $\widehat{u}(z)$ given by equation (37) with parameters $\epsilon_1 = 0.1$, $\epsilon_2 = 0.5$, $N = 3$. The last four figures, 11 ,12, 13, 14 depict the magnitude of the Fourier transform of the overall system using frequency averaging of the resulting deconvolution kernels depicted in figures 8 up to 10.

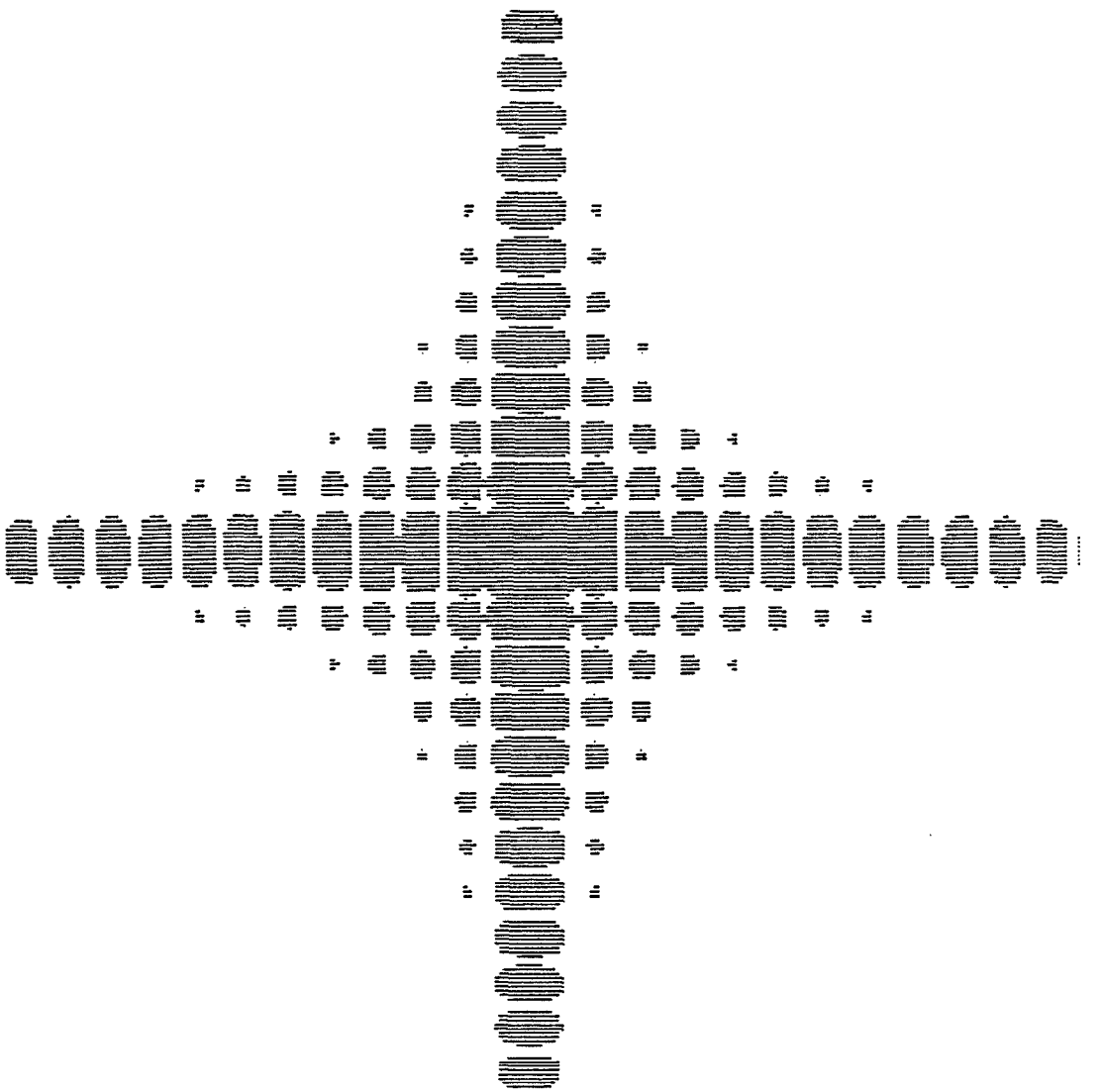

Figure 2: Magnitude of FT of convolver 1, t=0.1

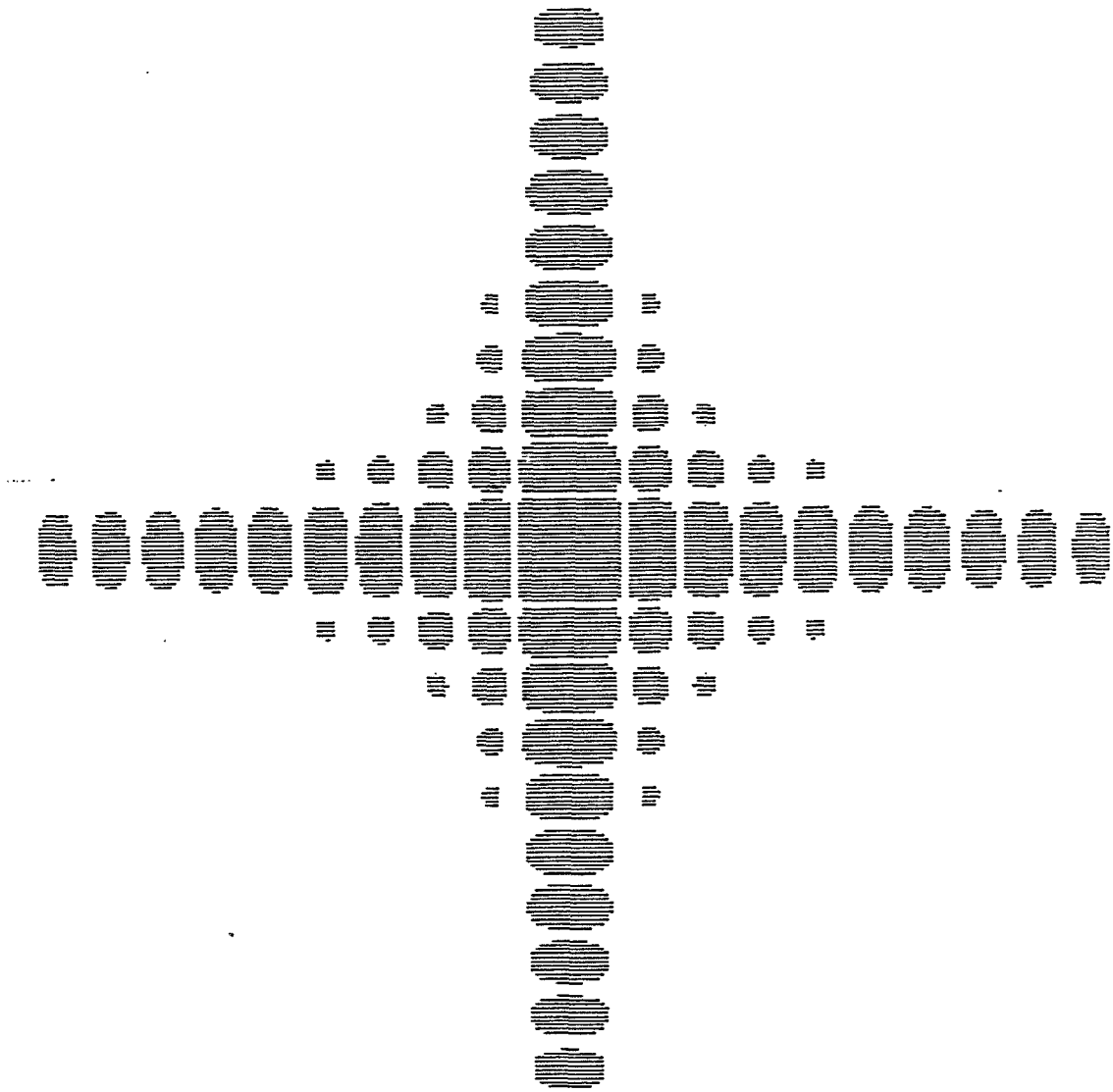

Figure 3: Magnitude of FT of convolver 2, t=0.1

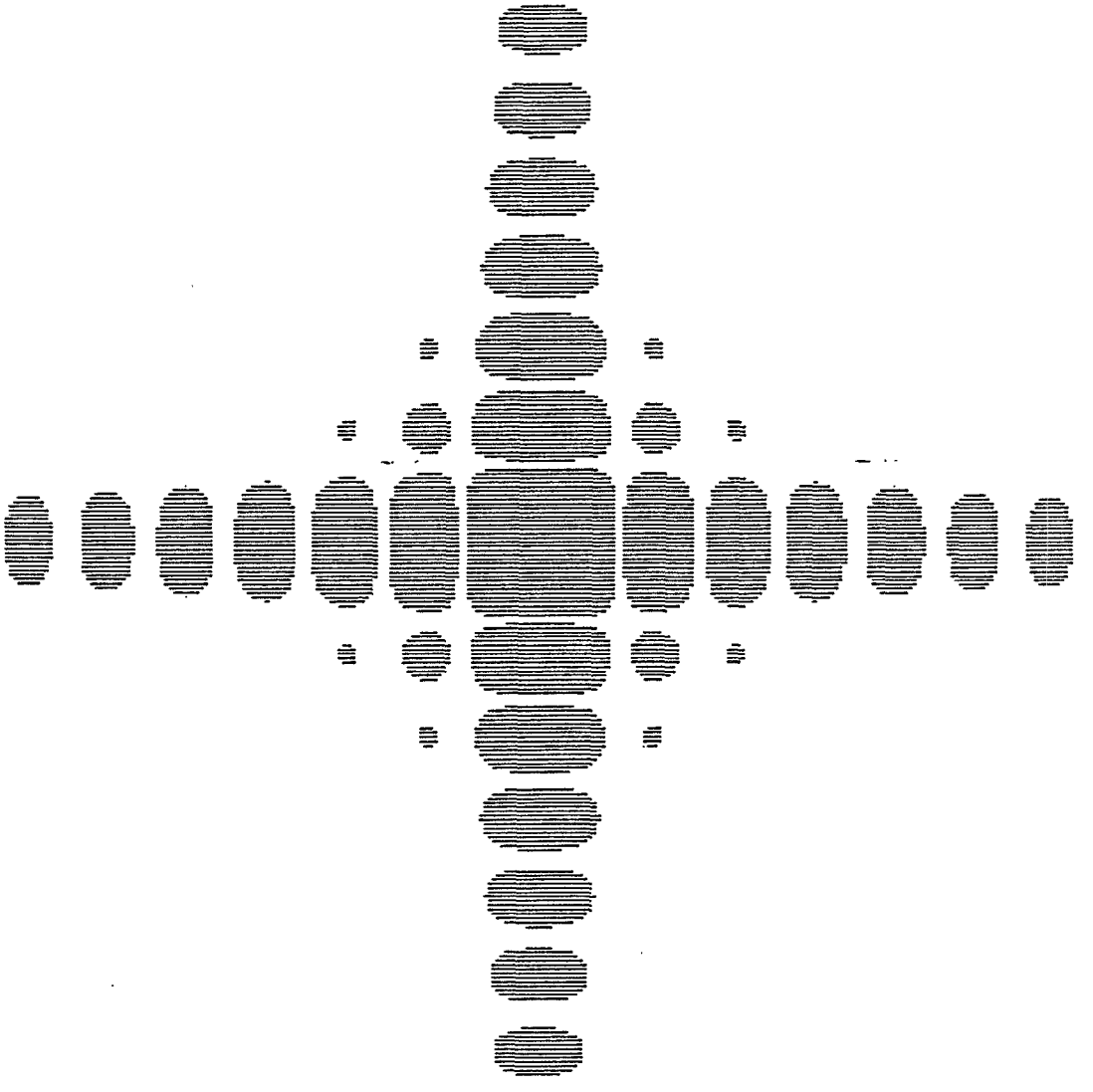

Figure 4: Magnitude of FT of convolver 3 (best one), t=0.1

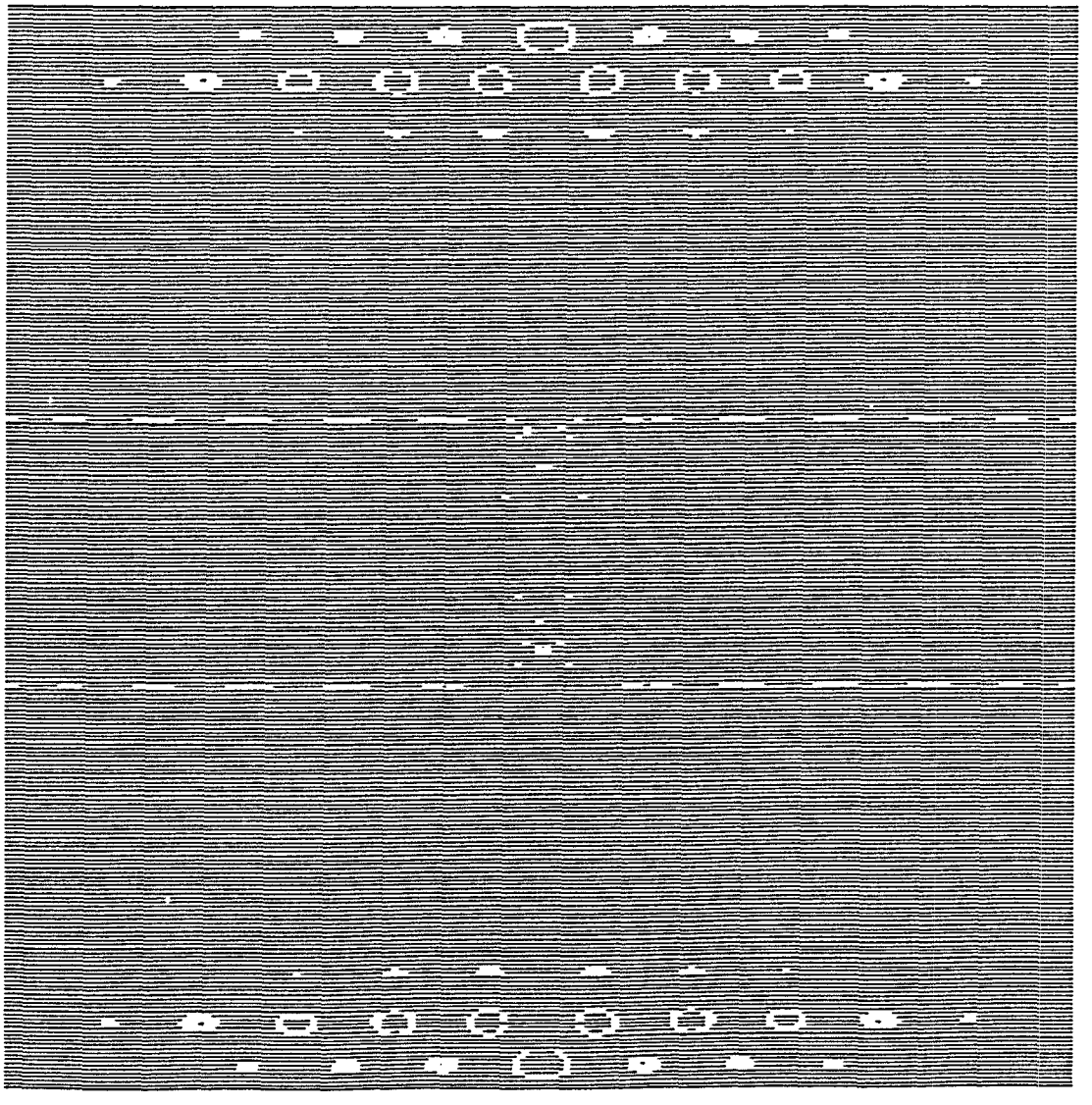

Figure 5: Magnitude of FT of overall system, $\epsilon = 0.1,\ N = 3,\ t = 0.1$

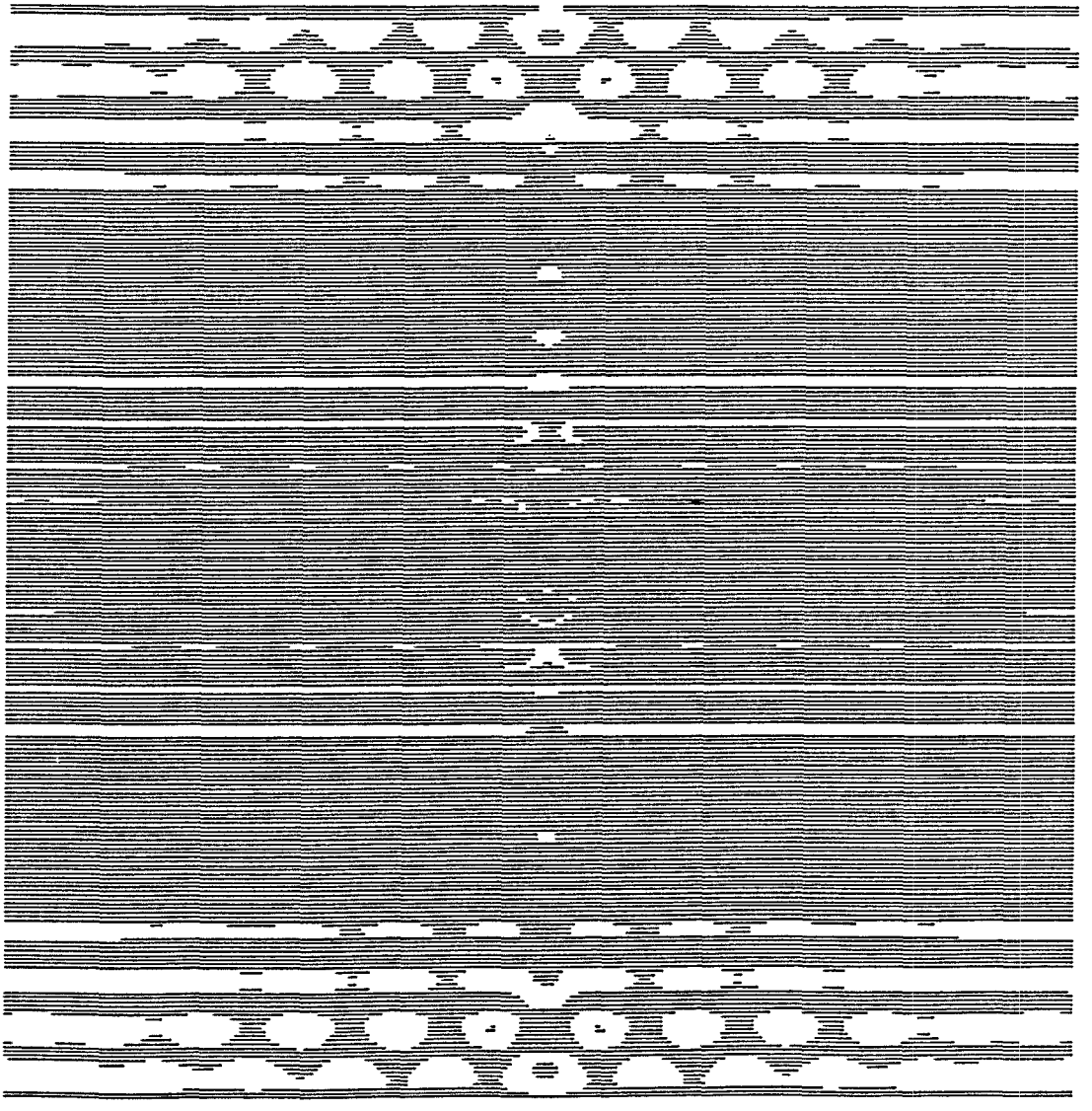

Figure 6: Magnitude of FT of overall system, $\epsilon = 0.1,\ N = 3,\ t = 0.5$

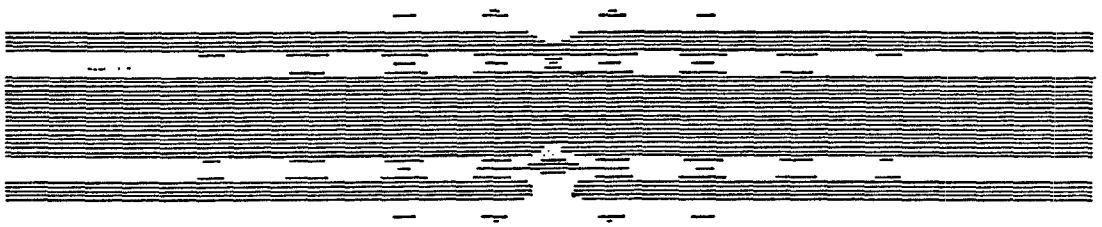

Figure 7: Magnitude of FT of overall system, $\epsilon = 0.1,\ N = 3,\ t = 5.0$

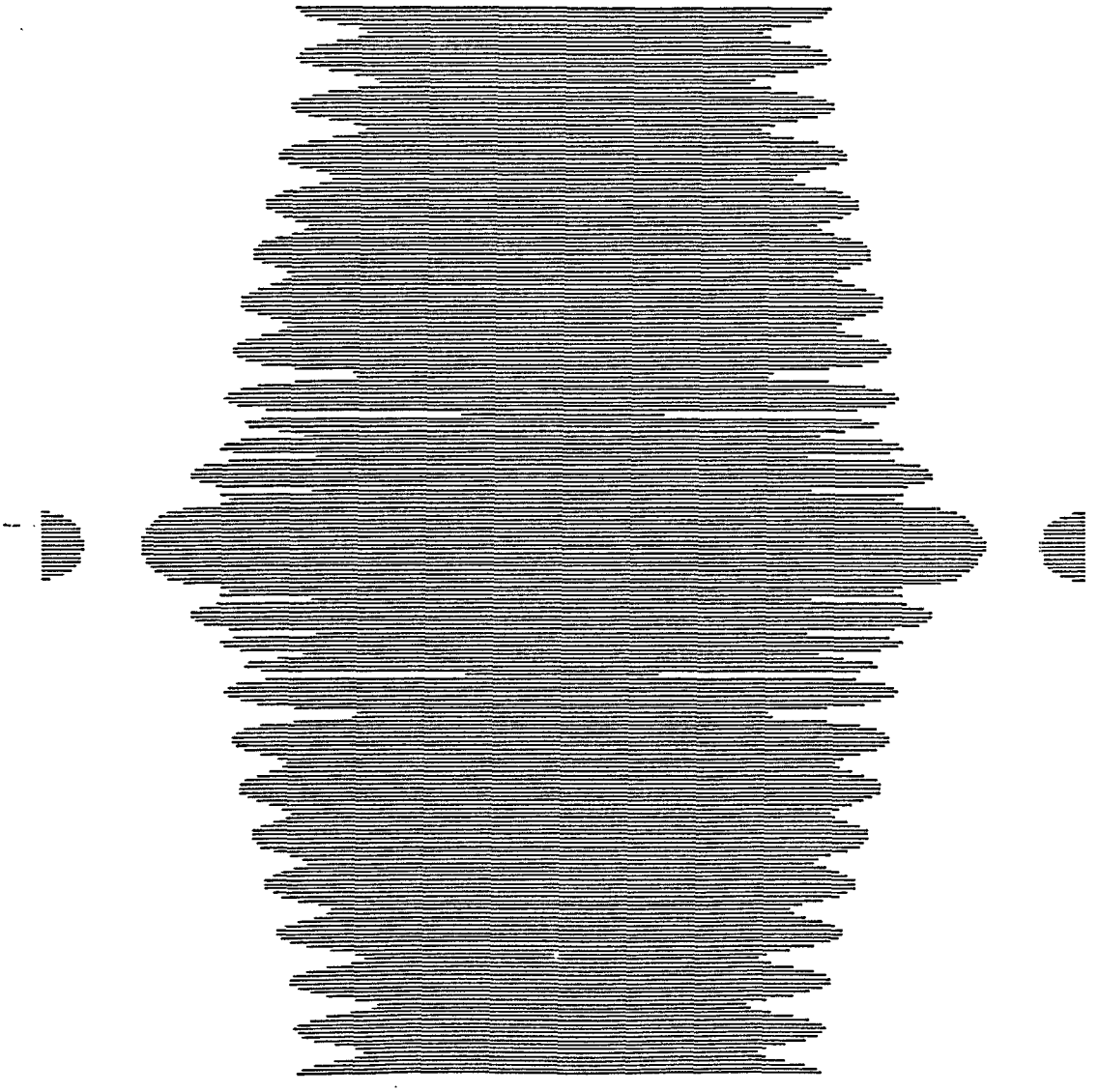

Figure 8: Magnitude of FT of overall system, $\epsilon_1 = 0.1,\ \epsilon_2 = 0.5,\ N = 3, t = 0.1$

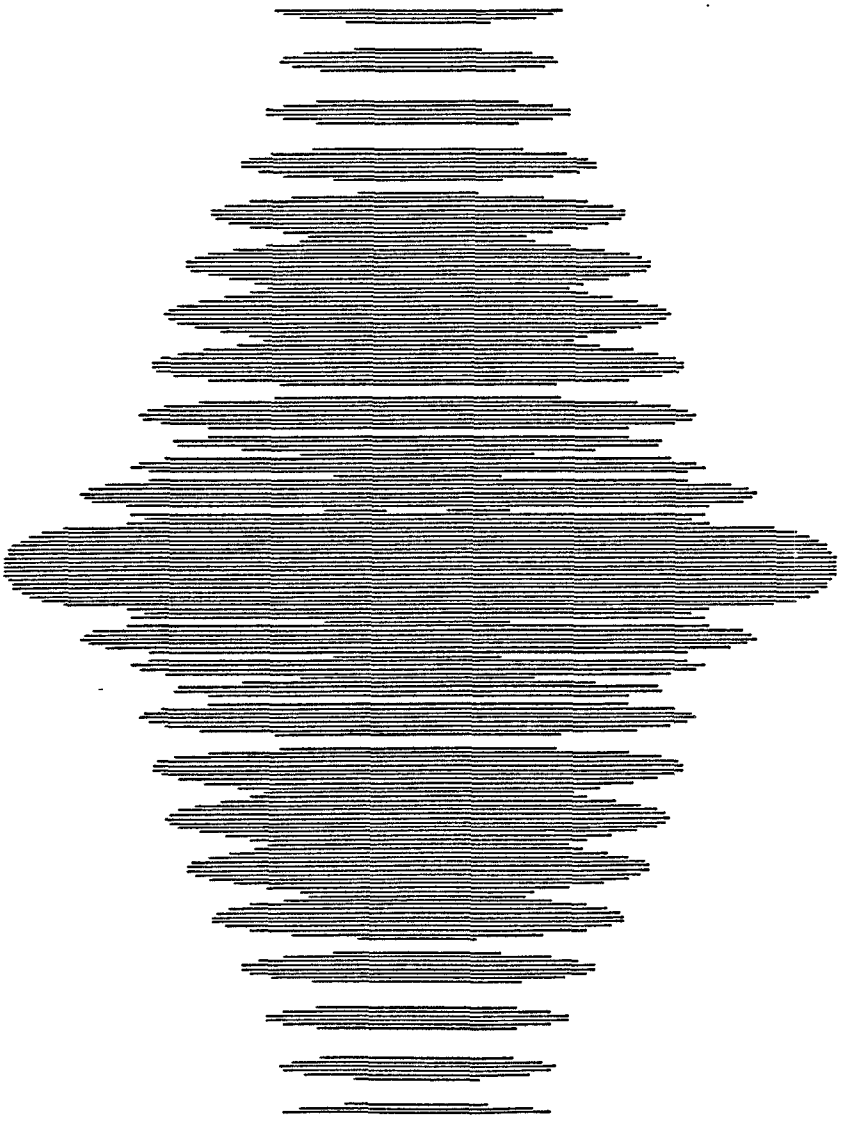

Figure 9: Magnitude of FT of overall system, $\epsilon_1 = 0.1$, $\epsilon_2 = 0.5$, $N = 3, t = 0.5$

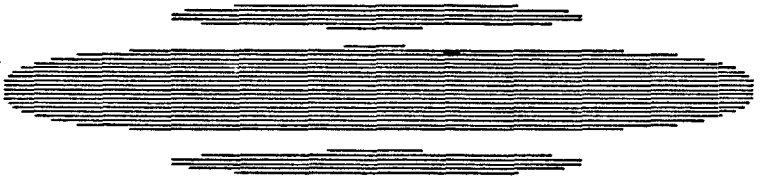

Figure 10: Magnitude of FT of overall system, $\epsilon_1 = 0.1$, $\epsilon_2 = 0.5$, $N = 3, t = 5.0$

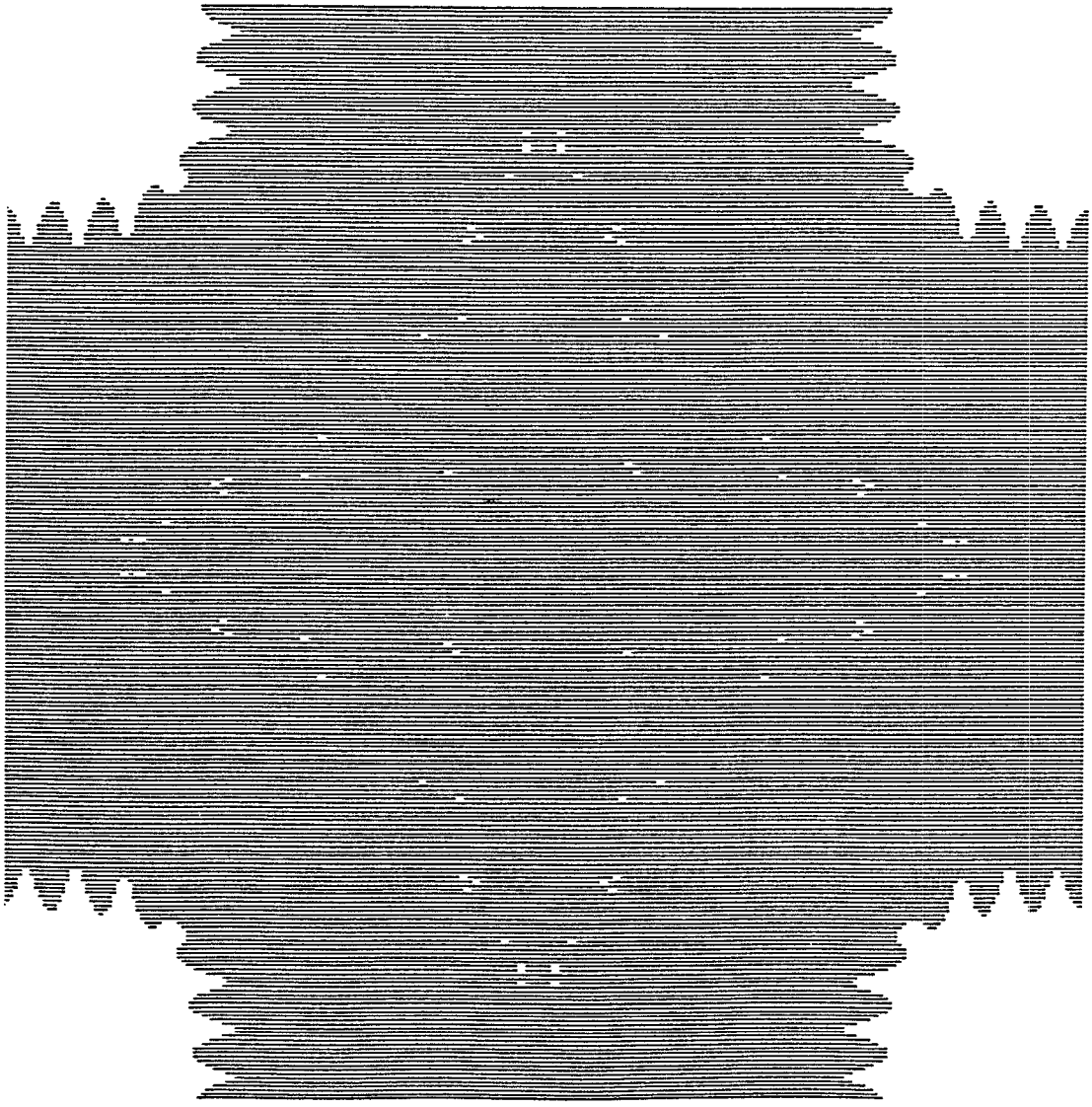

Figure 11: Magnitude of FT of overall system, $\epsilon_1 = 0.1$, $\epsilon_2 = 0.5$, $N = 3$, *averaged*, $t = 0.01$

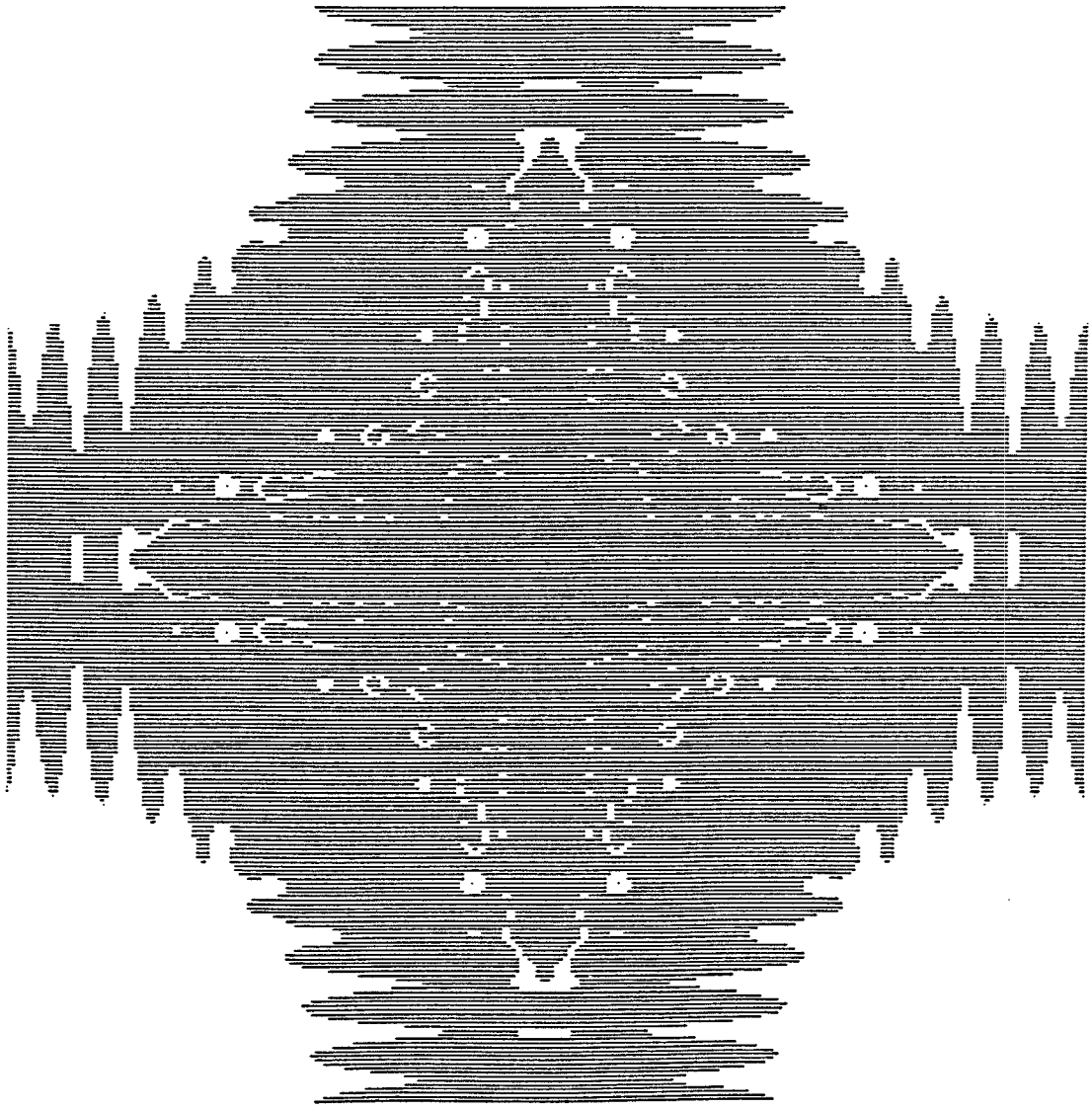

Figure 12: Magnitude of FT of overall system, $\epsilon_1 = 0.1$, $\epsilon_2 = 0.5$, $N = 3$, *averaged*, $t = 0.1$

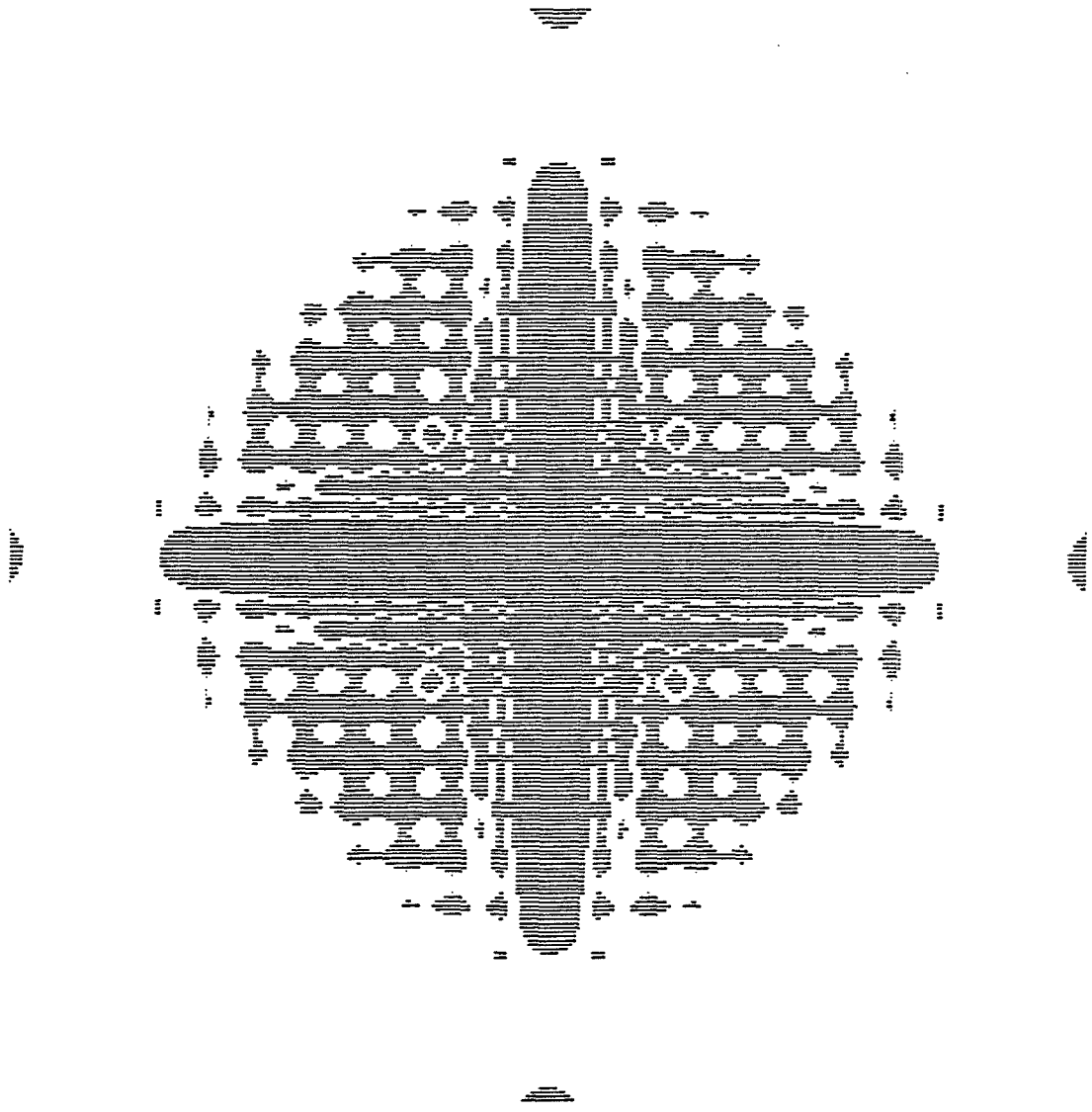

Figure 13: Magnitude of FT of overall system, $\epsilon_1 = 0.1$, $\epsilon_2 = 0.5$, $N = 3$, *averaged*, $t = 0.5$

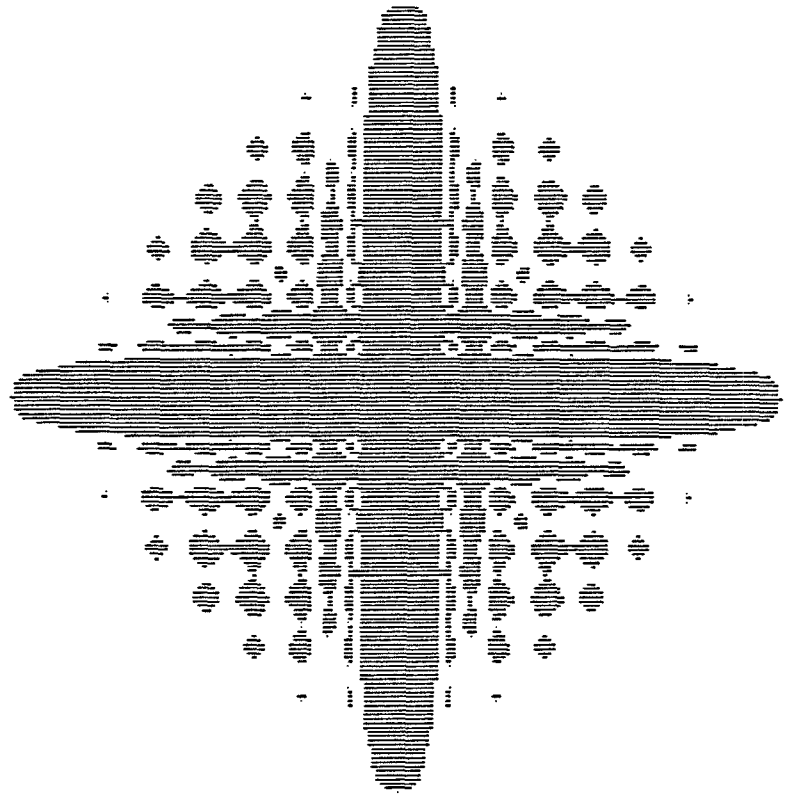

Figure 14: Magnitude of FT of overall system, $\epsilon_1 = 0.1$, $\epsilon_2 = 0.5$, $N = 3$, *averaged*, $t = 1.0$

3 Efficient Computation

A very important issue (at least from the point of view of applications) is how efficiently can "reasonably good" approximate deconvolution kernels be computed from raw data such as samples of the frequency response of the convolvers, or, ideally, analytic expressions for the convolution kernels or their Fourier transforms. There are several complex issues involved, including the basic questions of modeling, data availability, accuracy of measurements (resolution) and others. We will not discuss these issues here but we will assume that a sufficiently accurate model of the convolvers is available. Since we will work with *samples* of the Fourier transforms of the convolution kernels the data set will eventually be discrete. We remark however that the algorithm requires precise knowledge of the common zeros of the very well behaved subfamily (and is in fact sensitive to errors in the location of these common zeros).

As soon as a sufficient model has been established the actual computation seems quite straightforward; one basically needs to calculate pointwise approximations to an infinite sum, that is, approximate an infinite sum for every point over a finite two-dimensional grid of frequencies. For reasonable resolution and degree of approximation this computation can simply be overwhelming! A typical set-up for simulations throughout this work has been as follows: 256×256 individual frequencies and 3200 terms/point for each frequency. The computation of each term requires a relatively large number of floating point operations by itself. Therefore the task becomes time-consuming for an ordinary sequential machine, especially since one usually needs to apply a trial-and-error approach to optimize various parameters in order to meet design goals. Quite fortunately the problem at hand is inherently parallel in nature and renders itself for efficient implementation using a special machine architecture that exists commercially. The key observation is that the computation for each frequency point is independent from the corresponding computation for any other point.

3.1 The Data Parallel Architecture

The data parallel architecture is a combination of data parallel software and hardware that supports parallel data-element-wise processing of large *uniform* data structures, such as arrays or fields. Simply put, Data Parallel computing associates one processor with each data element. Upon instruction from the supervising central control unit, each processor operates on

its associated data element, i.e. all processors execute the *same* sequence of operations each on *its own* data element in a *synchronous* fashion. This computing style exploits the natural computational parallelism inherent in many data-intensive problems.

The particular machine used throughout this work has been the Thinking Machines Corp. Connection Machine CM-2 system. This is an advanced, highly sophisticated machine that supports the Data Parallel Computing model. Data parallel operations are implemented directly in hardware. In its full configuration the CM-2 system parallel processing unit contains 65,536 data processors, logically subdivided into four clusters of 16,384 processors each. Each data processor contains a separate Arithmetic and Logic Unit (ALU), 256 Kbits of bit-addressable local memory, an optional floating point accelerator, an I/O interface as well as a number of interprocessor communication interfaces. Arbitrary point-to-point communications are permitted by means of special-purpose hardware, called *The Router*. Message passing can occur in parallel; all processors can simultaneously send and receive messages via mailboxes that reside in their local memories. A finer system called *The NEWS Grid* implements a nearest-neighbor communication scheme that is much more efficient than the general router mechanism. The NEWS Grid is realized in hardware too. The Grid operates via a permutation circuit. This permutation circuit has another mode of operation, known as *Direct Hypercube Access* that facilitates the design of rather complex but quite regular communication patterns.

The data structure to be operated upon is uniformly spread over the data processor grid of one, two or four clusters. Each data element of the structure resides in the local memory of a data processor. If the data structure is bigger than the actual number of processors available (which is the normal case), a virtual processor mechanism becomes active. As a result each data processor is timeshared between two or more tasks and its associated local memory is sliced into a proportional number of equal-length segments. From the user point of view this process is transparent. Parallel extensions of the popular programming languages C, Fortran and Lisp are supported. The actual language extensions are minimal, depending on context to distinguish scalar from parallel operations. "Loaded" versions of all familiar functions and constructs are provided. These enable the use of a rather abstract programming style that does not require explicit identification of parallel operations.

3.2 Optimizing the computation of the deconvolution kernels - Grid Layouts

With the Connection Machine Data Parallel Architecture in mind, the next task is to optimize the target computation with respect to various efficiency considerations. Next we stress the most important facts that need to be taken into account, based on our model problem.

1. Symmetry of Deconvolution kernels in the transform domain. As a result we only need to compute the pointwise values of the corresponding Fourier transforms in the upper-right frequency quadrant.

2. For each frequency pair, (z_1, z_2), careful reshuffling of summation terms (over the nullset $\mathcal{Z}$) can result in a reduced number of required floating point operations.

3. For each frequency pair, (z_1, z_2), and each nullset point (ζ_1, ζ_2) the corresponding terms for the Fourier Transforms of the three deconvolvers *share a common factor.* Therefore this factor need only be computed once for all three uses. Recall that for $i = 1, 2, 3$ we have

$$\widehat{h}_i(z_1, z_2) = \sum_{(\zeta_1,\zeta_2)\in\mathcal{Z}} \frac{\widehat{u}(\zeta_1, \zeta_2)}{J(\zeta_1, \zeta_2)\widehat{f}_3(\zeta_1, \zeta_2)} \cdot \frac{C_i(z_1, z_2, \zeta_1, \zeta_2)}{(z_1 - \zeta_1)(z_2 - \zeta_2)} \qquad (56)$$

It is worth noting that this common factor carries out much of the computation involved. Hence *for a given point* (z_1, z_2) the computations $\widehat{h}_1(z_1, z_2)$, $\widehat{h}_2(z_1, z_2)$, $\widehat{h}_3(z_1, z_2)$ are *strongly related*; this fact can be effectively used to our advantage.

Fact (1) reduces the complexity by $\frac{1}{4}$. Fact (2) by a factor close to $\frac{1}{4}$. Fact (3) can result in reductions of up to $\frac{2}{3}$, depending on the floating point function library used. Hence the total gain is in the order of $\frac{2}{48} = \frac{1}{24}$.

Returning to the specific computing model and assuming "enough" processors what would be the most efficient thing to do? One can employ parallelism at various different levels. A very efficient way to attack the problem would be as follows: For each pair of frequencies, (z_1, z_2), in the upper-right transform quadrant assign *one data processor to each nullpoint* (ζ_1, ζ_2), and use the NEWS GRID nearest neighbor communication facility to compute partial sums row-wise along the grid. This scheme should be replicated for all three kernels and for all frequency pairs (z_1, z_2) in the upper right transform quadrant. The data processor grid layout would be as in figure 15, where $\bullet$ denotes a data processor, and $+$ denotes floating point

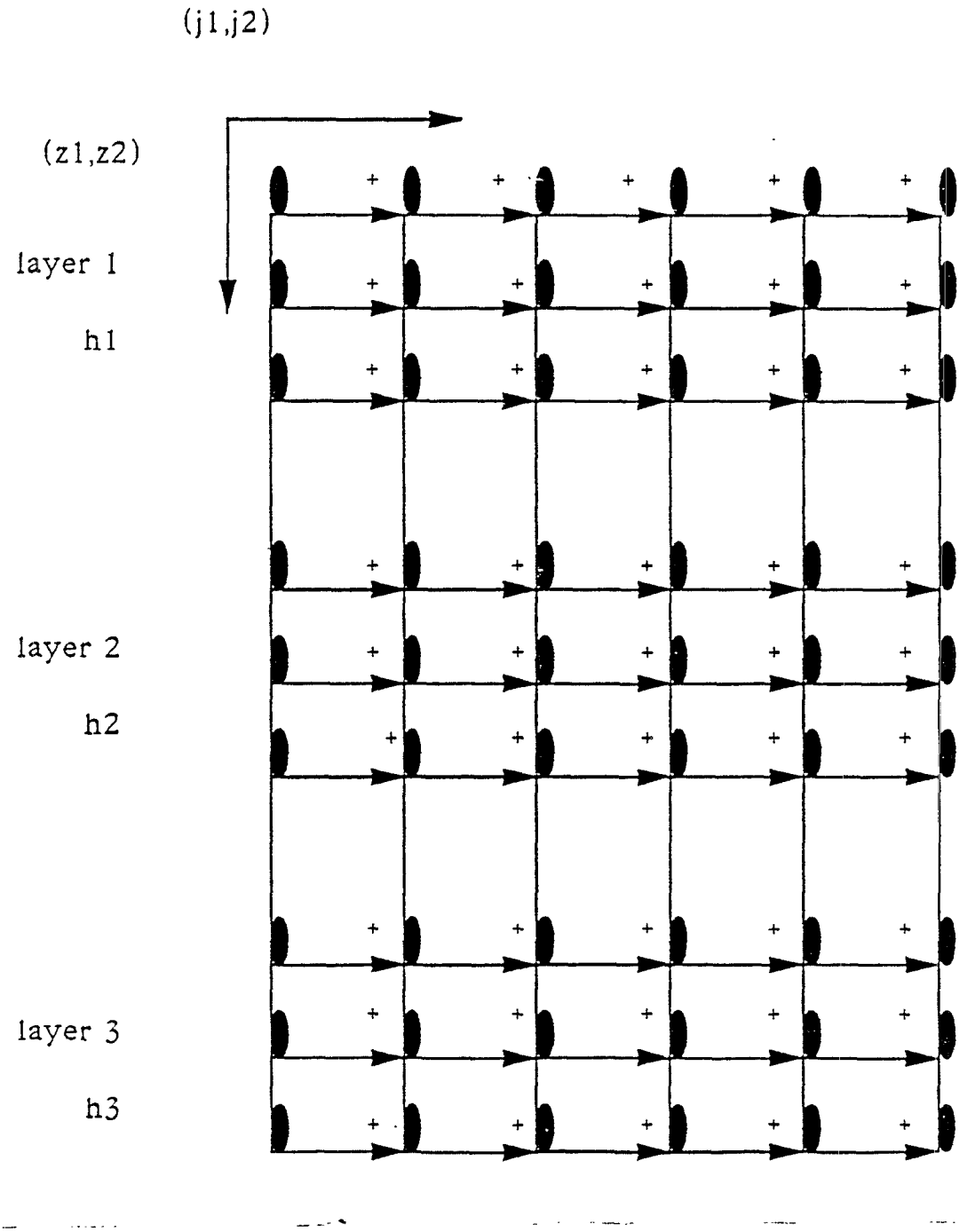

Figure 15: Layered grid configuration for distributed computation, Type I

addition. This grid configuration is *not optimal* in terms of time efficiency because it does not make use of Fact (3). Next we add a fourth computing layer that calculates the factor $\frac{\widehat{u}(\zeta_1,\zeta_2)}{J(\zeta_1,\zeta_2)\widehat{f}_3(\zeta_1,\zeta_2)}$ for each pair (ζ_1,ζ_2) of the nullpoint set and feeds the result to the appropriate computing cells. This scheme makes *partial use* of Fact (3). This time we need to introduce *vertical cell communications* to enable this new type of transaction to take place. This (type II) grid setup is depicted in figure 16, where $\bullet$ denotes a data processor, $\rightarrow$ denotes interprocessor communication, and $+$ denotes floating point addition. The grid operates as follows: While Layer O computes the factors $\frac{\widehat{u}(\zeta_1,\zeta_2)}{J(\zeta_1,\zeta_2)\widehat{f}_3(\zeta_1,\zeta_2)}$ the cells of Layers 1-3 compute the factors $\frac{C_i(z_1,z_2,\zeta_1,\zeta_2)}{(z_1-\zeta_1)(z_2-\zeta_2)}$. When both computations are completed a *column-wise parallel fetch transaction*, takes place after which each Layer 1-3 cell multiplies the fetched value with its result and then a *row-wise* $+$ *transaction* takes place. Results rest in the right most column. Both these strategies are highly efficient but require a very large number of virtual processors. This implies that each actual processor must be timeshared between a large number of tasks. Thus the task hopping rate increases and the cummulative overhead per computation cycle becomes significant. As a result system throughput is slowed down. Unless the number of actual processors is increased by an order of magnitude one needs to relax the computing power requirements. The proposed grid configurations, although currently impractical, have demonstrated the massively parallel nature of the problem. We now turn to a more modest strategy.

In its full configuration the Connection Machine model CM-2 employs 64K processors. With a frequency resolution of 512×512 points we can simply assign each processor the task of computing one point value for all three kernels. This requires $\frac{512\times512}{4} = 64\text{K}$ processors. This way *no interprocessor communication is needed* and the size of the nullset is of little practical importance, because it does not affect the number of processors required (only affects the execution time). Thus quite large nullsets can be easily accommodated. Notice that since each processor computes a specific point value *for all three kernels*, Fact (3) can easily be exploited. In a fully configured Connection Machine with 64K processors the run time (excluding I/O) is around four minutes (for the upper right hand quadrant only).

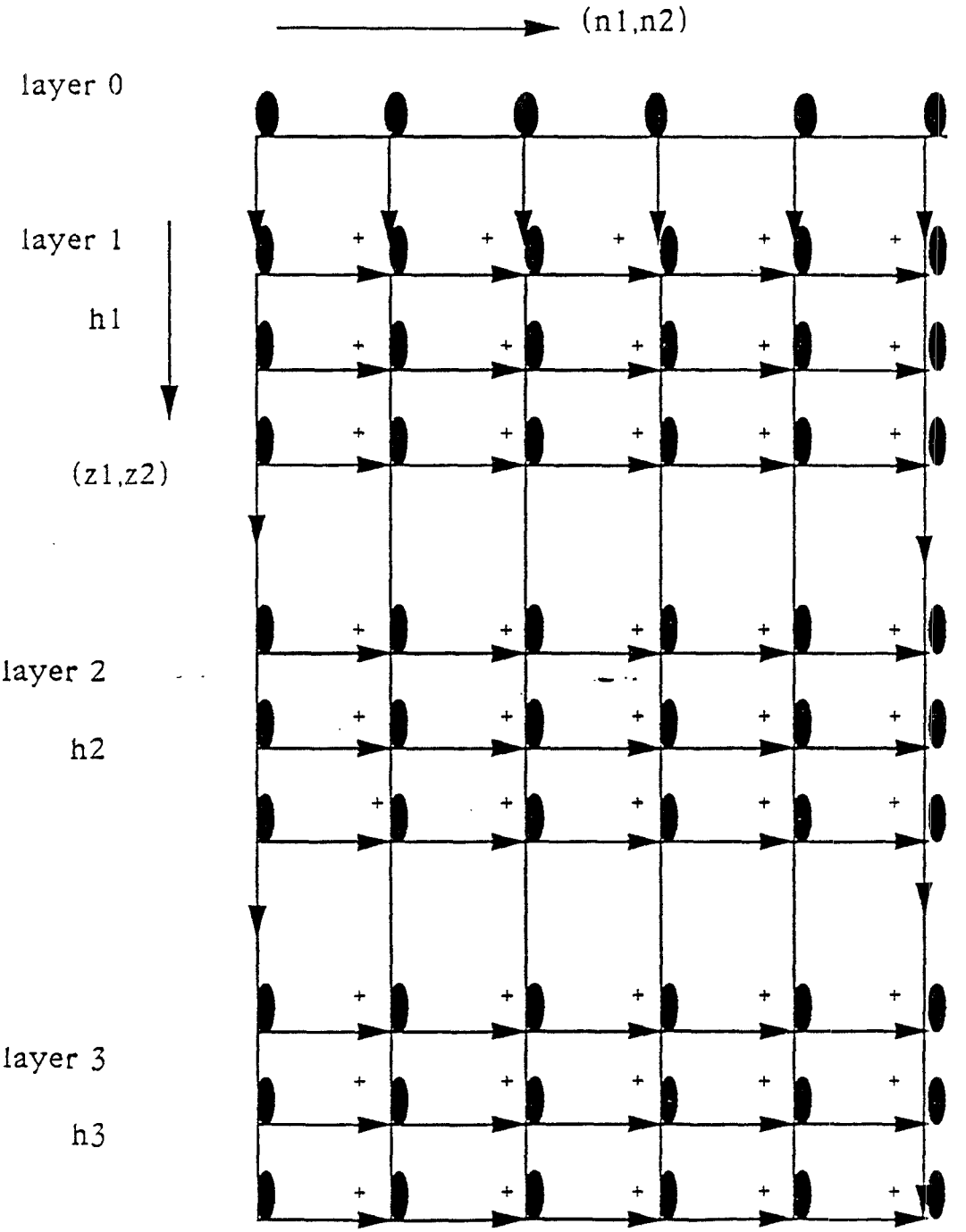

Figure 16: Layered grid configuration for distributed computation, Type II

4 Conclusions

We have described results on a specific solution to the two dimensional Analytic Bezout Equation. We have employed recent methods of complex analysis to obtain *compactly supported* deconvolution kernels. This is an important property for real-time filtering applications. The computability of reasonably good approximations to these ideal deconvolution kernels has been verified. These approximations are themselves compactly supported (but of support which is wider than that of the ideal kernels) and they permit arbitrarily good reconstruction of the original image. It has to be noted that these kernels are computed off-line and therefore the computational load involved is of no significance in so far as the applications are concerned. Nevertheless, since interactive design requires a trial-and-error approach the process can become time consuming. To overcome this difficulty we have proposed a number of Data Parallel grid layouts that are very efficient in performing the required computation and render themselves for fast implementation on commercially available machines.

Acknowledgements We are thankful to the University of Maryland Institute for Advanced Computer Studies (UMIACS) for the use of the Connection Machine, and to the technical support staff for some initial help with programing the Connection Machine.

References

[1] C. A. Berenstein, P. S. Krishnaprasad, and B. A. Taylor. Deconvolution methods for multisensors. Technical Report DTIC ADA 152351, University of Maryland, 1984.

[2] C. A. Berenstein and D. Struppa. On explicit solutions to the Bezout equation. *Systems Control Letters*, 4:33–39, 1984.

[3] C. A. Berenstein and D. Struppa. 1-Inverses for polynomial matrices of non constant rank. *Systems Control Letters*, pages 309–314, 1986.

[4] C. A. Berenstein and D. Struppa. Small degree solutions for the polynomial Bezout equation. *Linear Algebra Appl.*, 98:41–56, 1988.

[5] C. A. Berenstein, B. A. Taylor, and A. Yger. Sur quelques formules explicites de deconvolution. *J. Opt*, 14:75–82, 1983.

[6] C. A. Berenstein and A. Yger. Le probleme de la deconvolution. *J. Funct. Anal.*, 54:113–160, 1983.

[7] C. A. Berenstein and A. Yger. Ideals generated by exponential polynomials. *Adv. in Math.*, 60:1–80, 1986.

[8] C. A. Berenstein and A. Yger. Analytic Bezout Identities. *Advances in Applied Mathematics*, 10:51–74, 1989.

[9] B. Berndtsson. A formula for interpolation and division in C^n. *Math. Anal.*, 263:395–418, 1983.

[10] N. K. Bose. *Applied Multidimensional Systems Theory.* Reidel, Dordrecht, 1984.

[11] A. R. Davies, M. Iqbal, K. Maleknejad, and T. C. Redshaw. A comparison of statistical regularization and Fourier extrapolation methods for numerical deconvolution. In P. Deuflhard and E. Hainer, editors, *Proc. of Int. Workshop on Numerical Treatment of Inverse Problems in Differential and Integral Equations, Heidelberg FRG, Aug 30 - Sept 3, 1982*, Stutgart, 1983. Birkhauser.

[12] L. Ehrenpreis. *Fourier Analysis in Several Complex Variables.* Interscience. Wiley, New York, 1970.

[13] L. Hormander. Generators for some rings of analytic functions. *Bull. Amer. Math. Soc.*, 73:943–949, 1967.

[14] L. Hormander. *Linear Partial Differential Operators.* Springer-Verlag, Berlin, Heidelberg, New York, third edition, 1969.

[15] R. E. Molzon, B. Shiffman, and N. Sibony. Average growth estimates for hyperplane sections of entire analytic sets. *Math. Ann.*, 257:43–59, 1981.

[16] V. P. Palamodov. *Linear Differential Equations with Constant Coefficients.* Springer-Verlag, New York, 1970.

[17] E. V. Patrick. Deconvolution for the case of multiple characteristic functions of cubes in R^n. Technical report, Systems Research Center, University of Maryland, 1986.

[18] L. Schwartz. *Theorie des Distributions.* Herman, Paris, 1950.

[19] N. D. Sidiropoulos. Image Deconvolution Using Multiple Sensors. M.S. Thesis, Dept. of Electrical Engineering, University of Maryland, to appear as a Technical report, Systems Research Center, University of Maryland, 1990.

[20] D. Slepian. On Bandwidth. *Proc. of the IEEE*, 64(3), March 1976.

[21] S. A. Tretter. *Introduction to Discrete time Signal Processing.* Wiley, New York, 1976.